Journal of Thermal Stresses

ISSN: 0149-5739 (Print) 1521-074X (Online) Journal homepage: http://www.tandfonline.com/loi/uths20

# THE EFFECT OF WORK HARDENING ON THERMALLY INDUCED DEFORMATIONS IN ALUMINIUM DC CASTING

Ivar Farup, Asbjorn Mo

**To cite this article:** Ivar Farup, Asbjorn Mo (2000) THE EFFECT OF WORK HARDENING ON THERMALLY INDUCED DEFORMATIONS IN ALUMINIUM DC CASTING, Journal of Thermal Stresses, 23:1, 71-89, DOI: 10.1080/014957300280579

**To link to this article:** http://dx.doi.org/10.1080/014957300280579

Journal of Thermal Stresses, 23:71–89, 2000

0149-5739 /00 $12.00 + .00

# THE EFFECT OF WORK HARDENING ON THERMALLY INDUCED DEFORMATIONS IN ALUMINIUM DC CASTING

**Ivar Farup**
*SINTEF Materials Technology*
*Oslo, Norway*

**Asbjørn Mo**
*SINTEF Materials Technology*
*Oslo, Norway*

*This article documents a series of physical direct chill casting simulations performed on specimens of an AA3103 alloy by means of a Gleeble machine. During the experiments the specimens are subjected to thermal and straining histories similar to those experienced by material points in an ingot during the casting process due to thermal stresses. The measured stress is compared to the stress given by a steady-state creep law for the measured temperature and strain rate versus time. The creep law gives a good fit for temperatures above 400°C but increasingly overestimates the stress level as the temperature decreases below this level because of the increasing importance of work hardening. Since thermally induced straining occurs in the entire temperature interval in the casting process, it is concluded that more sophisticated constitutive modeling than the creep law is needed.*

During *direct chill* (DC) casting of aluminium, the ingot undergoes permanent deformations caused by the nonhomogeneous cooling contraction of the solidified metal [1]. In order to understand, optimize, and design the casting process, mathematical modeling based upon the conservation principles of continuum mechanics is intensively used. Important input to such modeling are the constitutive equations relating stress, strain rate, and temperature.

Different constitutive models have been applied for such modeling. Moriceau [2] and Janin [3] used a temperature-dependent elastoplastic model of the form $\sigma = \sigma(\varepsilon_p, T)$. A similar approach also incorporating creep using the so-called overlay concept [4] was used by Mathew and Brody [5]. Brody et al. [6] assumed

Received 21 September 1998; accepted 1 December 1998.

Terje Iveland and Ola Gikling, Hydro Aluminium R&D Centre, Sunndalsøra, Norway, are greatly acknowledged for their assistance during the experiments. The authors also thank Hallvard Fjær, IFE, Norway, for providing temperature and strain histories for the casting process obtained by modeling and for valuable suggestions on the manuscript. This research was funded by Hydro Aluminium, Elkem Aluminium, Hydro Raufoss Automotive Research Centre, and the Research Council of Norway through the project PROSMAT—Støperikompetanse.

Address correspondence to Mr. Ivar Farup, Research Scientist, SINTEF Materials Technology, P.O. Box 124 Blindern, N-0314 Oslo, Norway.

steady-state creep behavior, i.e., $\sigma = \sigma(\dot{\varepsilon}_p, T)$, in their analysis. Fjær and Mo [7] developed the finite element model ALSPEN in which viscoplastic deformation was modeled by a modified Ludwig constitutive law on the form $\sigma = \sigma(\dot{\varepsilon}_p, \varepsilon_p, T)$ [8]. A similar material law was used in the model developed by Magain et al. [9]. Sample and Lalli's [10] constitutive model with one internal variable representing isotropic hardening was used by Smelser and Richmond [11] for the computation of air gap formation. This constitutive model, as well as a modified version of Miller's MATMOD equations [12], was also implemented in the three-dimensional version of ALSPEN [13]. Based on the ABAQUS software, Drezet and Rappaz [1] recently developed a three-dimensional mathematical model in which the steady-state creep law according to Garofalo [14] was applied to describing the solid state; the semisolid state was described by a Norton–Hoff creep law.

Although constitutive models with different degrees of sophistication have been used to model the DC casting process, it is not thoroughly documented whether, or in which manner, effects of work hardening influence the results. It is also unclear how they should be modeled mathematically. Mo and Holm [15] compared the MATMOD equations with the so-called "traditional approach" in which the material is described by representative stress-strain curves of the form $\sigma = \sigma(\dot{\varepsilon}_p, \varepsilon_p, T)$. By calculating the stress level for strain and temperature histories relevant for DC casting using both models, they concluded that one of the main shortcomings of the traditional approach is that the accumulated effective viscoplastic strain is regarded as a state variable and that kinematic hardening and recovery are neglected. Their results also indicated that the kinematic hardening can be important if the loading is reversed at a late stage in the process, that is, at low temperatures (below 250°C).

Nedreberg [8] carried out tensile tesing of the AA6063 alloy for temperatures from room temperature to 600°C and strain rates relevant for the DC casting process. According to her results, the steady-state creep regime is reached after a few percent of straining at 400°C and almost immediately at 500°C and above. Modeling results (see, e.g., [16]) indicate that viscoplastic straining at temperatures above 400°C gives a significant contribution to the total deformations occurring during the casting process. This result along with the fact that simulation models of the DC casting process based upon a simple creep law gives good agreement with experimental castings when determining the deformations of the ingot (see, e.g., [1, 17]) motivate an investigation into whether effects of work hardening can be neglected in modeling the casting process, at least for temperatures above a certain value.

In [18] the authors reported creep tests carried out for an as-cast AA3103 aluminium alloy by means of a Gleeble machine.[1] The present article documents a series of Gleeble experiments in which the AA3103 specimens are subjected to thermal and straining histories similar to those experienced by material points during the DC casting process. The results of these physical casting simulations are then discussed in terms of material strengthening mechanisms and existing constitutive models.

[1] Gleeble is a registered trademark of Dynamic Systems Inc.

## EXPERIMENTS

The Gleeble machine is used for the thermomechanical testing of metallic alloys. The specimen is heated by the Joule effect, and water-cooled steel jaws assure a high heat extraction at each side. Thus, only a small section at the center is held at the prescribed temperature, and the stress and strain rate vary in the axial direction of the specimen due to the temperature dependency of the flow stress. To ensure that the position of maximum straining really is at the specimen center at which the controlling thermocouple is fixed, a slightly curved specimen geometry as indicated in Figure 1 is applied. Although the specimen geometry is noncylindric and the temperature inhomogeneous, the authors argued in [19, 18] that the diameter change measured at the center of the specimen by an extensometer can be used to determine the strain and strain rate when the specimen is subjected to small strains.

The length of the specimen (initially 90 mm between the jaws) was chosen to obtain the low strain rates, characteristic for thermally induced deformations in DC casting. The continuous change of temperature during the experiments caused the length of the specimen to change continuously due to thermal expansion. Since the resulting elongation is of the same or higher order of magnitude as the elongation needed for imposing the small strain rates characteristic for DC casting, the experiments were carried out with a prescribed force instead of a prescribed jaw velocity.

The experiments were performed on specimens of the AA3103 alloy (see Table 1 for composition) in the as-cast conditions. The specimens were prepared from the same ingot as was used for the experiments reported in [18]. To ensure that the mechanical properties were unchanged, four of the experiments from the series reported in that reference were repeated, and the results were all well within the measuring uncertainty. The creep law reported in that reference is thus representative of the steady-state creep behavior of the material used in this work in the temperature range 325°C to 550°C.

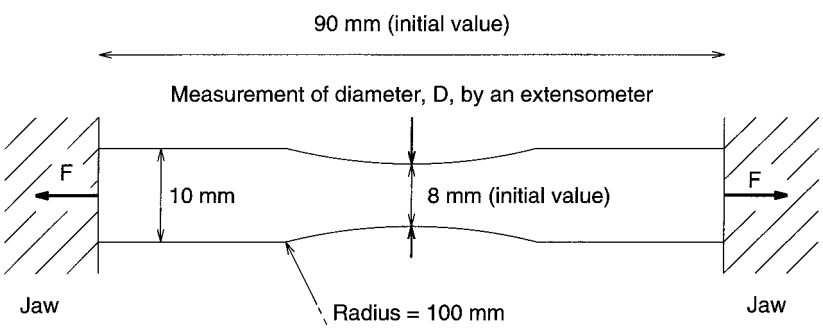


**Figure 1.** Gleeble specimen with circular cross section. Only the free part of the specimen is shown, and $F$ is the axial force at the jaws.

**Table 1 Composition (wt%) of the AA3103 alloy investigated in the present study**

| Fe | Si | Mg | Mn |
|---|---|---|---|
| 0.4928 | 0.0720 | 0.0035 | 1.0496 |

Based upon the DC casting simulation results [20] and the creep law reported in [18], three histories of corresponding temperature and force to be used as input to the Gleeble experiments were established. The three cases are labeled **A**, **B**, and **C** and are chosen to resemble representative histories of temperature and effective viscoplastic straining of material points in the ingot as follows:

**A**. *Central part of the ingot*: The temperature decreases linearly from 600°C to 300°C in 660 sec, and the effective viscoplastic strain rate is in the range $1-5 \times 10^{-5}$ sec$^{-1}$.
**B**. *Between center and short face of the ingot*: The temperature decreases from 600°C to 300°C in 60 sec. The strain rate in this period is in the range $5-10 \times 10^{-5}$ sec$^{-1}$.
**C**. *Close to long face*: The temperature decreases from 600°C to 200°C during 200 sec. During the first 100 sec, the effective viscoplastic strain rate is of the order $5 \times 10^{-5}$ sec$^{-1}$, whereas no straining occurs the next 100 sec. After this rapid cooling the temperature decreases from 200°C to 150°C in 200 sec, during which period the strain rate is of the order $2 \times 10^{-5}$ sec$^{-1}$.

Cases **A** and **B** are very similar in the respect that the specimen is continuously subjected to straining during the experiment. Their major difference is the cooling rate and the total amount of straining, which is larger in case **A** (similar strain rate, longer duration). In case **C** the material is unstrained between 400°C and 200°C, and during this period the material has the possibility to recover from any hardening imposed at higher temperatures.

In addition, two cases labeled **D** and **E** without any reference to the DC casting process were constructed. In these, the effect of straining at a high temperature (above 500°C) on the flow stress at a slightly lower temperature (between 400°C and 500°C) can be studied

**D**. The temperature decreases from 600°C to 400°C in 200 sec, and the strain rate is of the order $5 \times 10^{-5}$ sec$^{-1}$ through the entire experiment.
**E**. As case **D** except that no straining is imposed above 500°C.

The temperature and force histories given as input to the Gleeble machine for these five cases are illustrated along with the results, and the number of parallel experiments conducted for each case is summarized in Table 2. To determine experimentally the thermal strain associated with the temperature history alone, all the experiments were also carried out with zero applied force, hence referred to as

**Table 2 Number of parallel experiments for the five experimental cases**

| Case **A** | Case **B** | Case **C** | Case **D** | Case **E** |
|---|---|---|---|---|
| 4 | 5 | 3 | 2 | 2 |

*zero force experiments*. Here, only two parallel tests were conducted because of the high reproducibility.

## RESULTS

During the experiments, the force in the axial direction as well as the diameter and temperature at the center were measured as functions of time and recorded each second. As an example on the raw data, the measured diameter as a function of time is shown in Figure 2*a* for an experiment of case **A** and its corresponding zero force experiment.

From the zero force experiments the volumetric thermal straining of the specimen was determined as

$$\varepsilon_{\mathrm{T}}(t) = \ln \frac{D(t)}{D_0} \tag{1}$$

where $D(t)$ and $D_0$ denote current and initial diameter, respectively. For cases **A**–**E**, the effective axial stress, $\sigma$, and viscoplastic strain, $\varepsilon_p$, were determined as

$$\sigma(t) = \frac{F(t)}{A(t)} \tag{2}$$

$$\varepsilon_p(t) = 2\left[\varepsilon_{\mathrm{T}}(t) - \ln \frac{D(t)}{D_0} - \frac{\nu\sigma(t)}{E}\right] \tag{3}$$

where $F$, $A$, $\varepsilon_{\mathrm{T}}$, $E$, and $\nu$ denote the measured force, current cross-section area, thermal strain derived from corresponding zero force experiment, Young's modulus, and Poisson's ratio, respectively. The values for the latter two material constants as functions of temperature were taken from [21]. In Figure 2*b* the thermal and viscoplastic strains for the same case as depicted in Figure 2*a* are shown. For comparison the thermal strain was also determined directly from the measured temperature as

$$\varepsilon_{\mathrm{T}}(t) = \frac{1}{3} \ln \frac{\rho(T_0)}{\rho(T(t))} \tag{4}$$

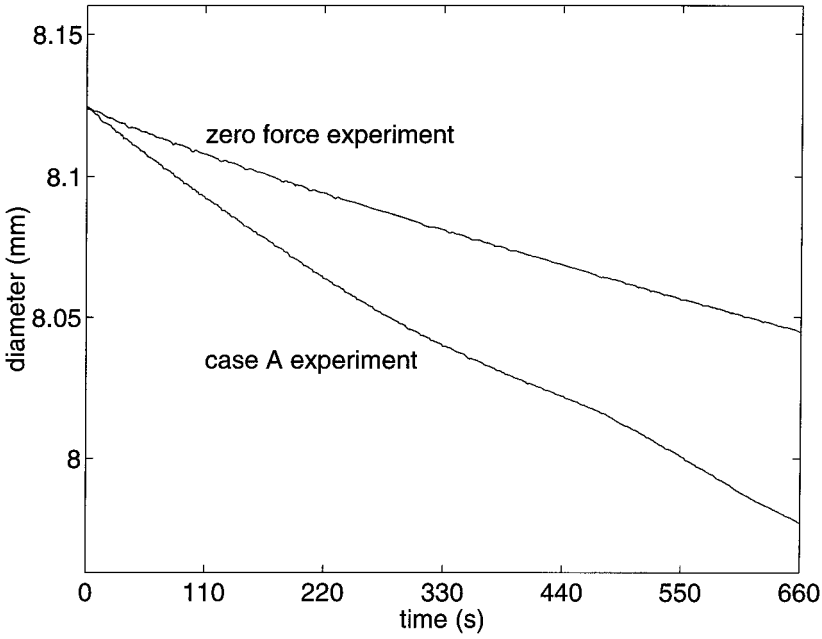


(a)

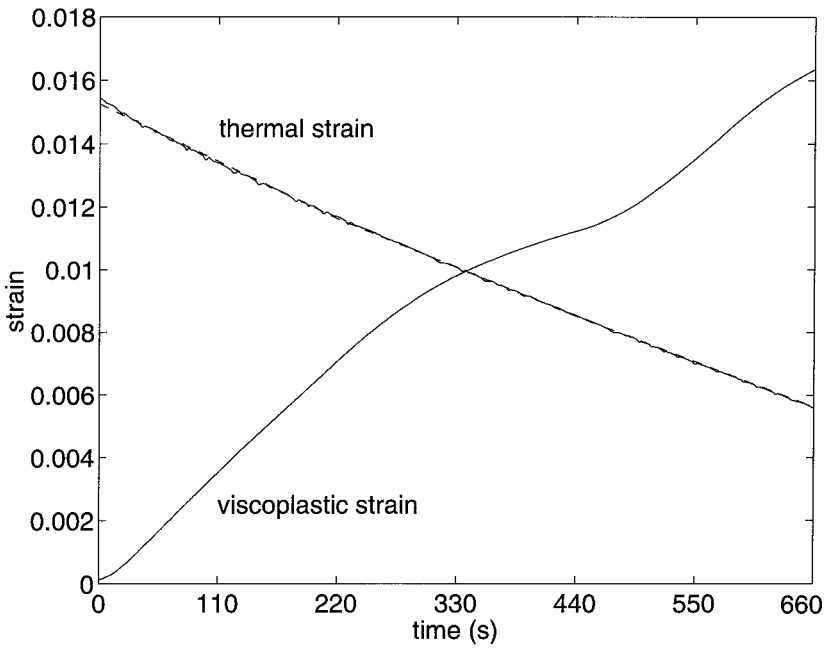


(b)

**Figure 2.** (*a*) Measured diameter *versus* time for a case **A** experiment and the corresponding zero force experiment. (*b*) Determined viscoplastic strain and thermal strain *versus* time for the same experiment. For a comparison the thermal strain as determined directly from the temperature and tabulated densities of pure aluminium is shown (dashed line).

where the density of pure aluminium as a function of temperature was taken from [22], and the two methods were found to give similar results (see Figure 2*b*). Using the preceding expressions, the stress state is tacitly regarded as uni-axial. The authors argued in [19, 18] that the error imposed by this simplification is small compared to the measuring uncertainty and the inherent difference between the specimens.

The viscoplastic strain was then filtered by means of moving averaging and differentiating numerically in order to obtain the effective viscoplastic strain rate, $\dot{\varepsilon}_p(t)$. From this viscoplastic strain rate and the measured temperature, $T(t)$, the "steady-state creep stress", $\sigma_c$, was determined from Garofalo's equation for steady-state creep as reported in [18],

$$\sigma_c(t) = \sigma_0 \sinh^{-1}\left\{\left[\frac{\dot{\varepsilon}_p(t)}{A}\exp\left(\frac{Q}{RT(t)}\right)\right]^{1/n}\right\} \tag{5}$$

where the temperature, $T$, is measured in Kelvin, and the parameters are listed in Table 3. If the effects of work hardening are negligible, the straining can be considered as steady-state creep and the calculated creep stress should be equal to the measured stress.

In Figures 3 to 5 the measured stress is plotted along with the stress calculated by the creep law. It should be noted that the creep stress as well as the measured stress were determined for each of the parallel experiments from the measured viscoplastic strain rate and that the mean values for these quantities are shown in the figure as functions of time. The standard deviation is below 1% for the measured stress and below 4% for the calculated stress.

## DISCUSSION

Comparing the measured stress with the stress calculated by the steady-state creep law (see Figures 3 to 5), it is seen that they correspond closely for temperatures above 400°C. The misfit for temperatures above 400°C is due to the misfit between the creep law and the actual steady-state creep behavior (see Figure 5 in [18]). This applies particularly to temperatures above 550°C, since no steady-state creep experiment was carried out in this range. As the temperature decreases below 400°C, the creep law increasingly overestimates the stress level, as is clearly observed in cases **A**, **B**, and **C**. The most obvious explanation for these observations is that the steady-state creep regime is reached almost immediately at high

**Table 3 Parameters in Garofalo's equation for the steady-state creep of AA3103**

| $A$ | $Q/R$ | $\sigma_0$ | $n$ |
|---|---|---|---|
| $1.33 \times 10^{16}\ \text{sec}^{-1}$ | 29012K | 31.6 MPa | 7.94 |

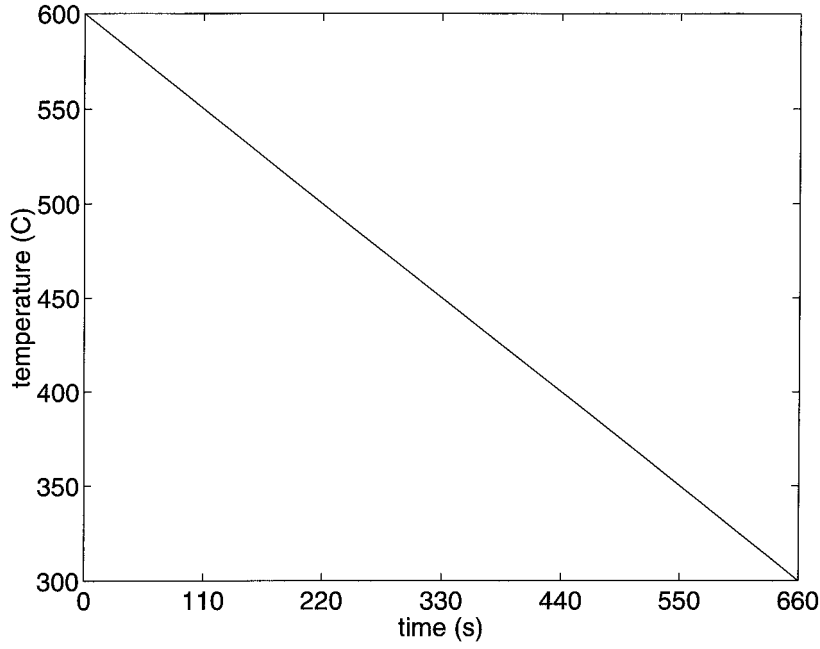


(a)

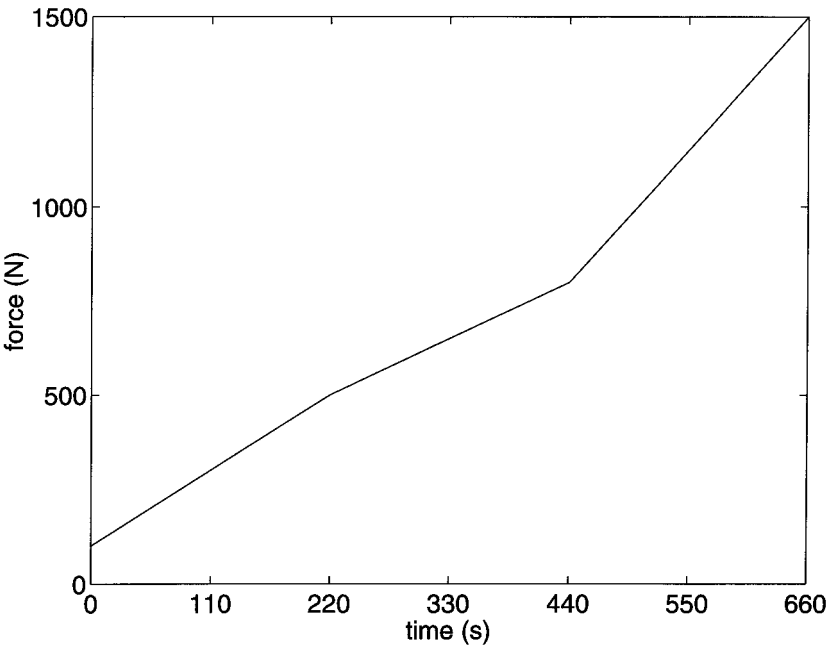


(b)

**Figure 3.** Input and results for cases *A* (a–c) and *B* (d–f).

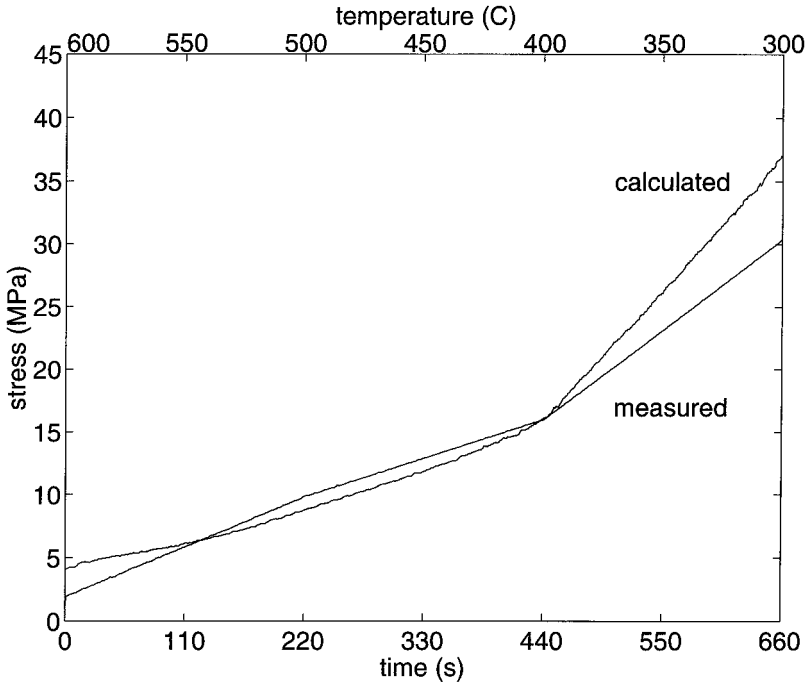


(c)

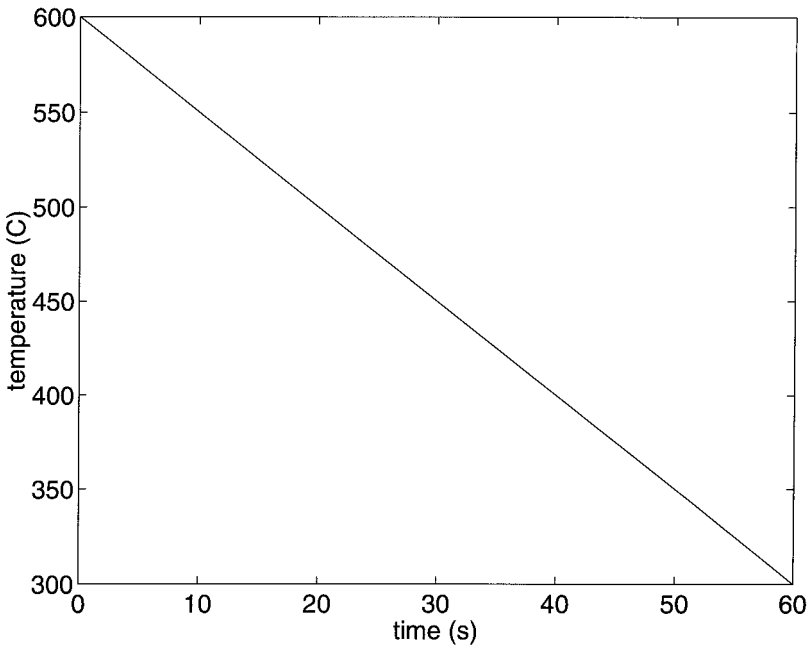


(d)

**Figure 3.** Input and results for cases *A* (a–c) and *B* (d–f) (*Continued*).

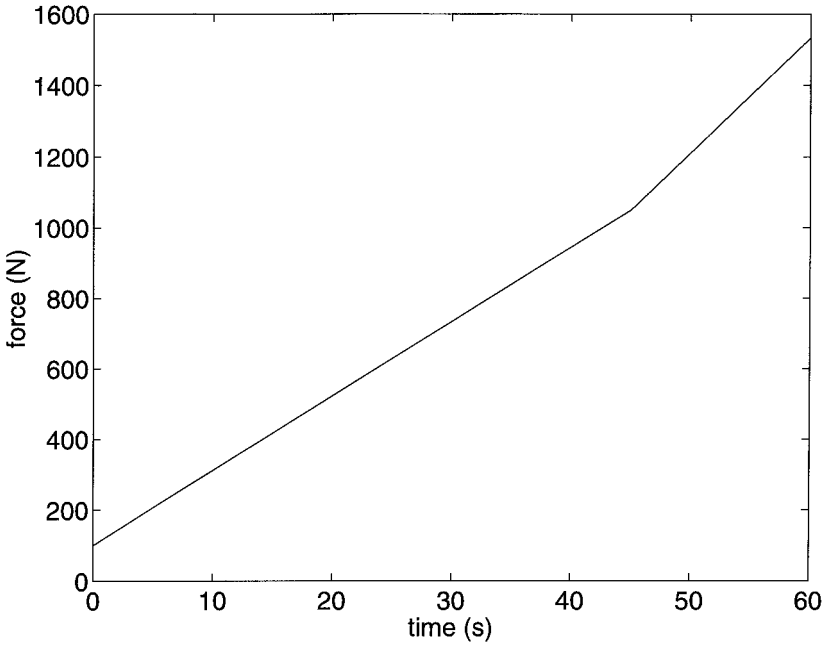


(e)

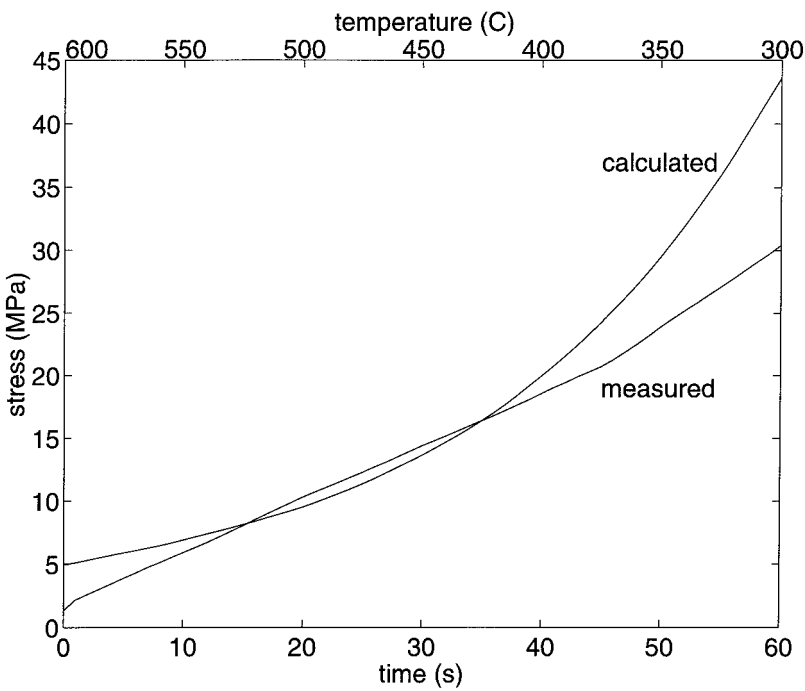


(f)

**Figure 3.** Input and results for cases *A* (a–c) and *B* (d–f) (*Continued*).

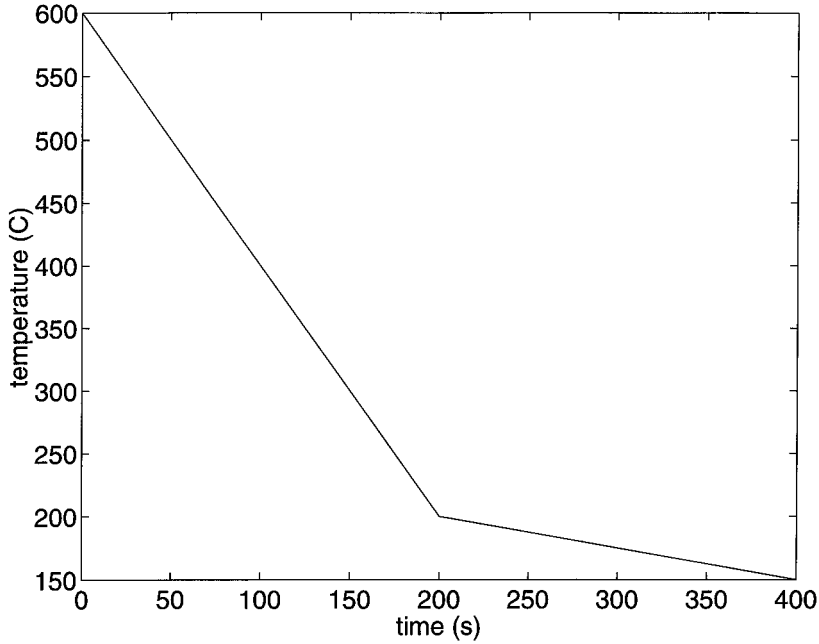


(a)

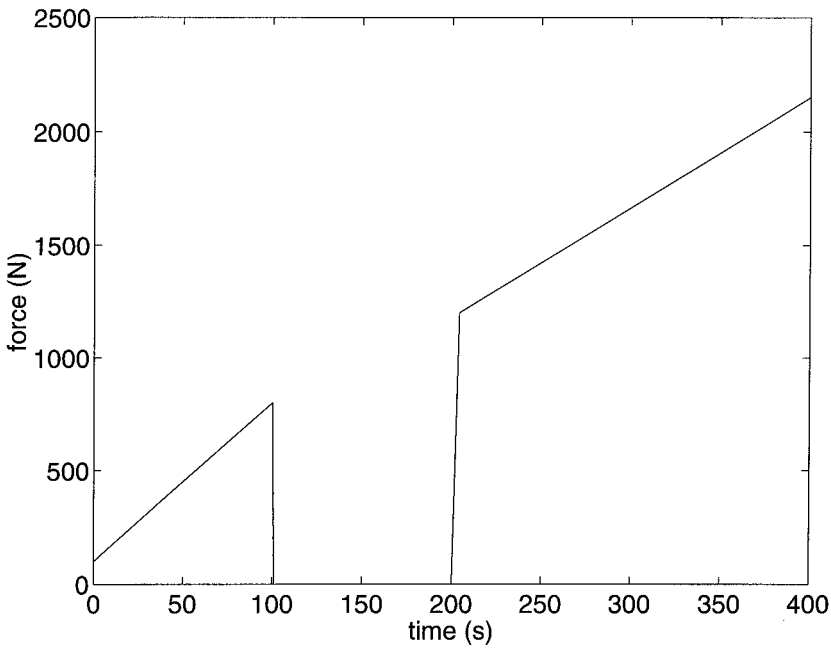


(b)

**Figure 4.** Input and results for case *A* (a–c) and *B* (d–f).

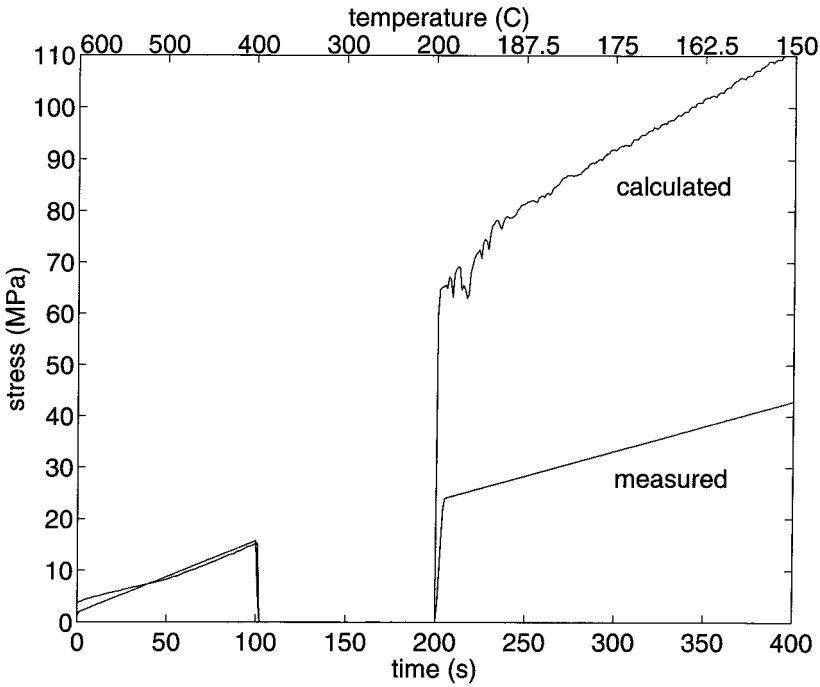


(c)

**Figure 4.** Input and results for case **C** (*Continued*).

temperatures, whereas significant straining is needed in order to obtain steady-state conditions at lower temperatures.

Several mechanisms contribute to the strength of an aluminium alloy, although not all of them change significantly during the casting process. The grain size, upon which the flow stress depends via the Hall–Petch relation (see, e.g., [23]), is constant during the process; and neither recrystallisation nor the formation of subgrains occurs as a result of the small strains involved [15]. The strength also depends significantly on the number and size of precipitates (particle hardening) and the amount of alloying elements in the solid solution. It was, however, argued in [15] that the cooling rate in the DC casting is so high that the elements remain in the solid solution during the entire process and that the effects of secondary precipitation can be neglected. This is particularly so for the AA3103 alloy investigated in the present study because of the low concentration of alloying elements and the low diffusivity of manganese in aluminium. Thus, the effects of grain size, foreign atoms in the solid solution, and particles upon the mechanical strength are accounted for by alloy-dependent material constants.

The remaining mechanism influencing the strength of the material is hardening due to the development of a dislocation configuration during straining. This phenomenon is commonly divided into two different parts, namely, isotropic and

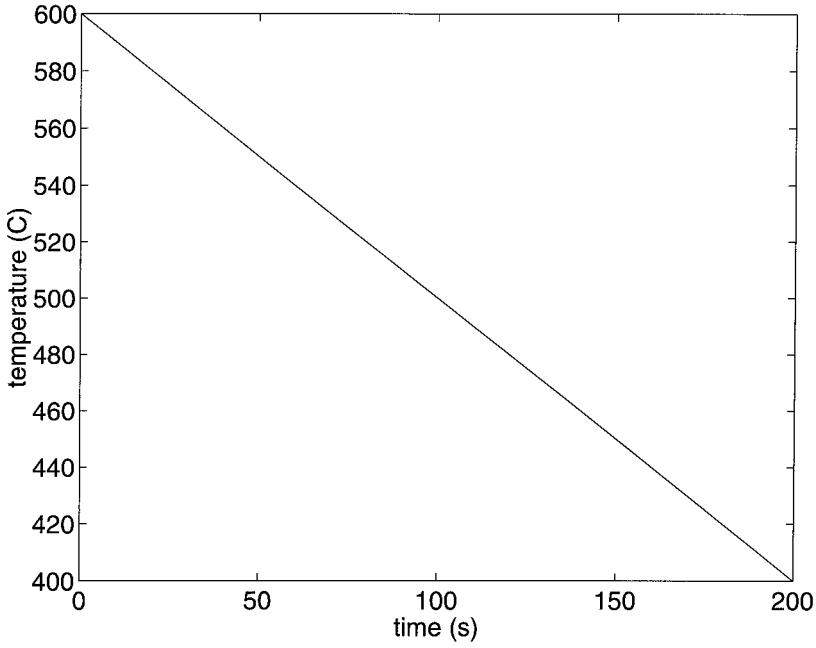


(a)

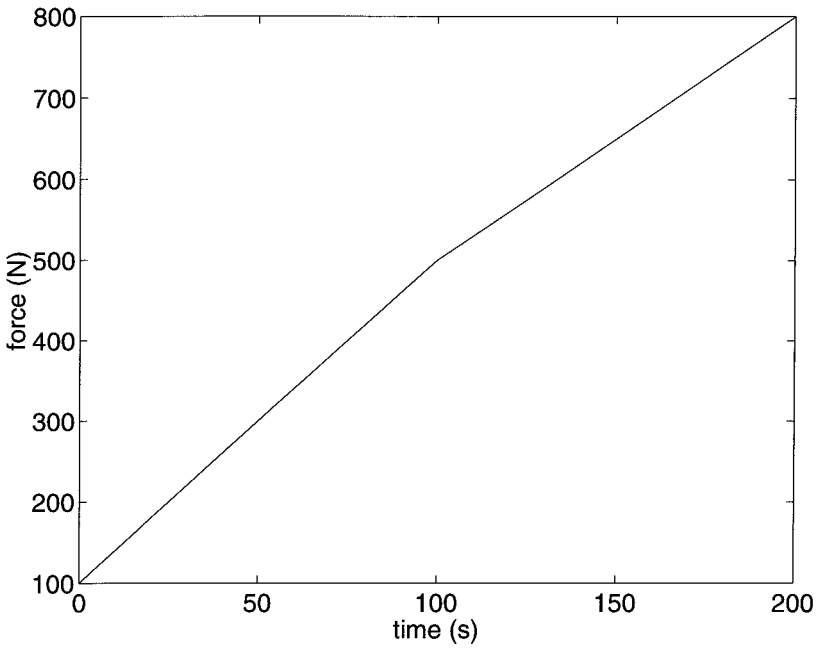


(b)

**Figure 5.** Input and results for cases **D** and **E**.

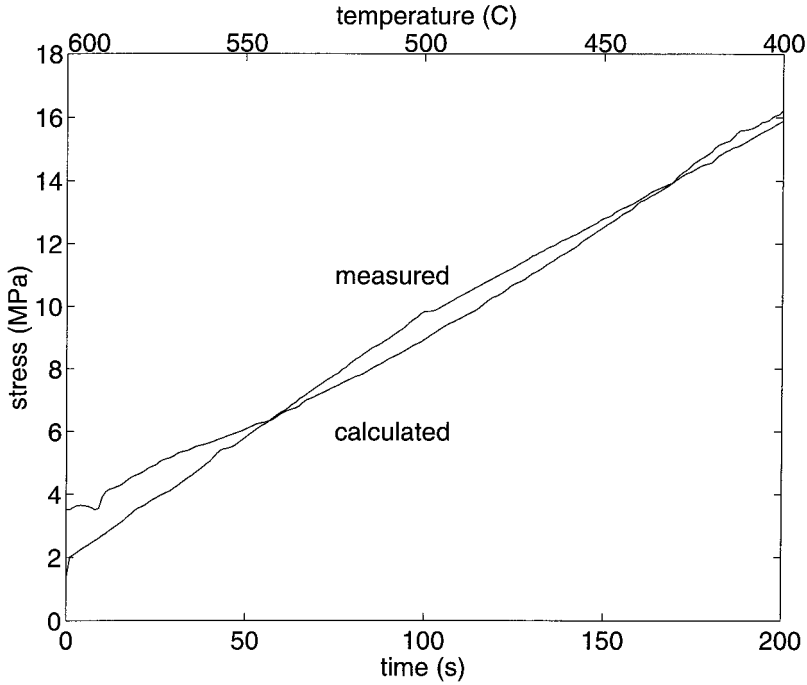


(c)

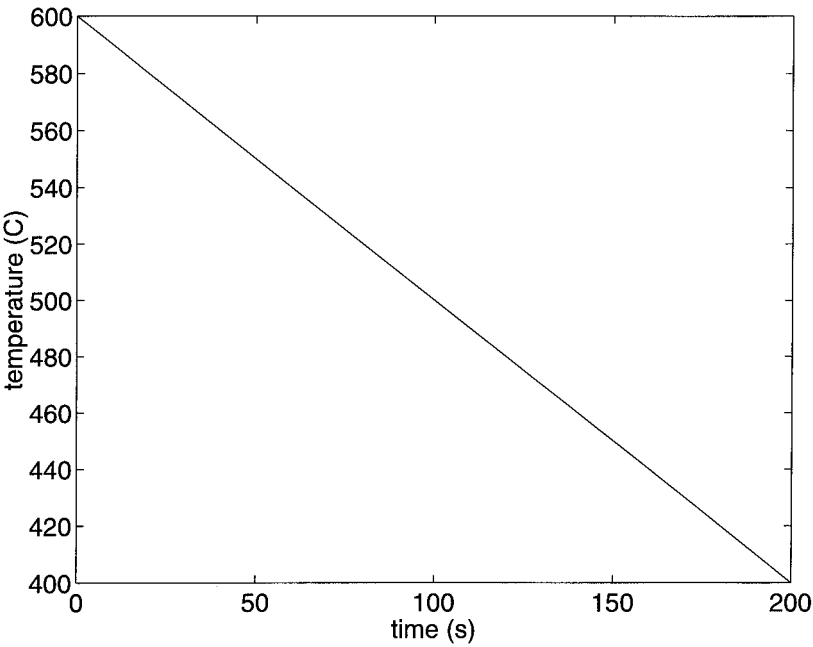


(d)

**Figure 5.** Input and results for cases **D** and **E** (*Continued*).

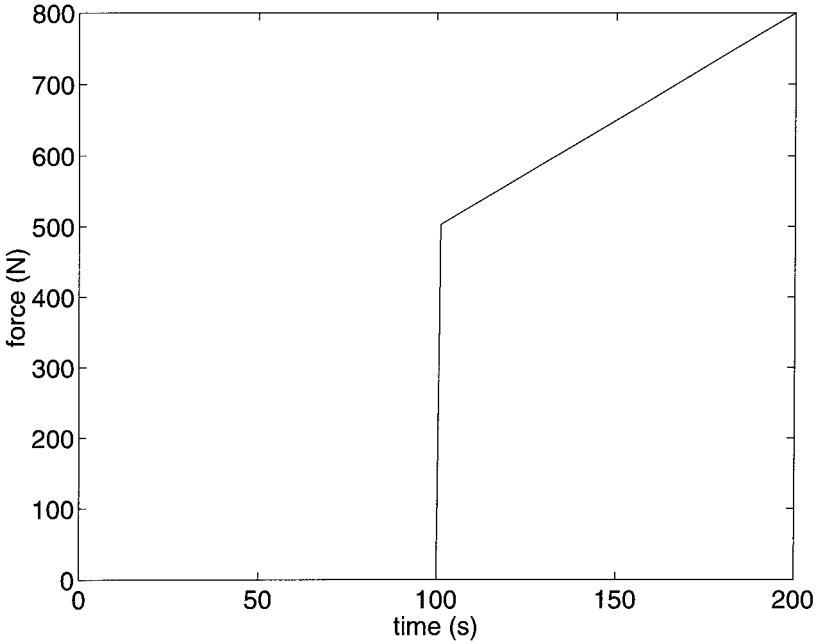


(e)

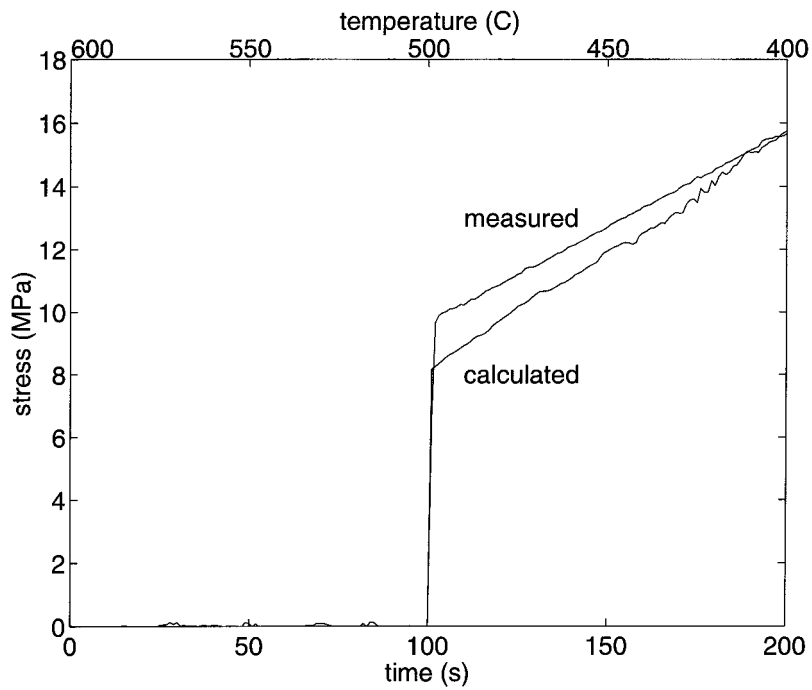


(f)

**Figure 5.** Input and results for cases **D** and **E** (*Continued*).

kinematic hardening. In constitutive models the isotropic hardening is usually represented by a scalar internal variable whereas the kinematic, anisotropic hardening is represented by a tensor. Effects of kinematic hardening are most clearly observed when the direction of loading is reversed, and it was argued by Mo and Holm [15] that this actually happens at some locations in the ingot during casting. However, since the major purpose of the present study is to investigate whether work hardening plays a significant part in the casting process at all, no experiment with reversed loading was performed.

While strain hardening is due to an increase in the dislocation density, recovery is caused by annihilation of dislocations. Such annihilation is mainly governed by self-diffusion of aluminium atoms and climb of dislocations. It is thus a thermally activated mechanism, and the recovery is a function of temperature and current dislocation density. If the dislocation density becomes very high, as it does when the material is exposed to large plastic deformation, further straining may enhance annihilation of dislocations. This effect, which is commonly referred to as dynamic recovery, is not important for thermally induced deformations because of the small strains involved. The annihilation is acting very fast at high temperatures, and equilibrium between strain hardening and thermal recovery is established rapidly when the material is strained. Steady-state creep is therefore the dominating deformation mechanism in this range. At lower temperatures, on the contrary, the annihilation mechanism is slow. Thus, large strains, and thereby also large dislocation densities, are needed to obtain the equilibrium between creation and annihilation of dislocations characteristic of steady-state creep.

These mechanisms are elucidated by the experiments. In case **A** the stress level at 300°C is 82% of the steady-state stress level, whereas in case **B** it is only 70%, indicating that the thermomechanical history is becoming important. For illustrative purposes the experiments in case **C** have been carried out for even lower temperatures, and it is observed that the discrepancy between the creep law and the measured stress continues increasing. Although the creep law was fitted to experiments carried out at 325°C and above, preliminary experiments at 250°C indicate that the creep law rather under- than overestimate the steady-state stress for temperatures below 325°C. In cases **D** and **E**, on the other hand, the stress level at 400°C to 500°C is (within the measuring uncertainty) unaffected by the straining history at temperatures above 500°C. In other words, the diffusion of annihilations is so fast that an equilibrium between creation and annihilation is reached almost immediately.

From the present study it is evident that above 400°C the flow stress can be related to the viscoplastic strain rate and the temperature by a steady-state creep law. It is furthermore evident that the creep law overestimates the stress level at lower temperatures. Since modeling results indicate that significant straining occurs also in this range at some locations in the ingot [20], the approach used by Brody et al. [6] and Drezet and Rappaz [1]—that is, to apply a creep law for the entire temperature interval—will give unreliable results for temperatures below 400°C; so more sophisticated constitutive modeling is needed. A fairly simple solution is to use a creep law at high temperatures and to introduce hardening

abruptly below a certain temperature, e.g., 400°C. This approach was applied in, for example, [7, 9].

Another possibility is to apply internal variable models such as the MATMOD equations [12] or the model of Sample and Lalli [10]. There are, however, some problems associated with this approach as well. If the parameters of such models are fitted so that the steady-state behavior at high temperatures and the hardening at low temperatures are well reproduced, the hardening transient at high temperatures becomes too extensive. As an illustration, stress-strain curves obtained by integrating the modified MATMOD equations used in [13] are shown in Figure 6. In the figure, the stress level is normalized by its steady-state value. It is observed that steady-state conditions are reached after as much as 2% straining at 400°C when the strain rate is $10^{-4}$ $sec^{-1}$, and thereby the flow stress for temperatures above 400° can be underestimated by as much as a factor of two. For these temperatures the model will also predict a strong history dependence, which is not observed in the experiments (cf. cases **D** and **E**).

In a real casting situation, thermally induced viscoplastic straining will begin as soon as the so-called coherency temperature is reached in the mushy zone. However, in accordance with the creep behavior between 400°C and 600°C observed in the present study, there is no reason to believe that the straining at temperatures above the solidus will affect the rheological behavior below this

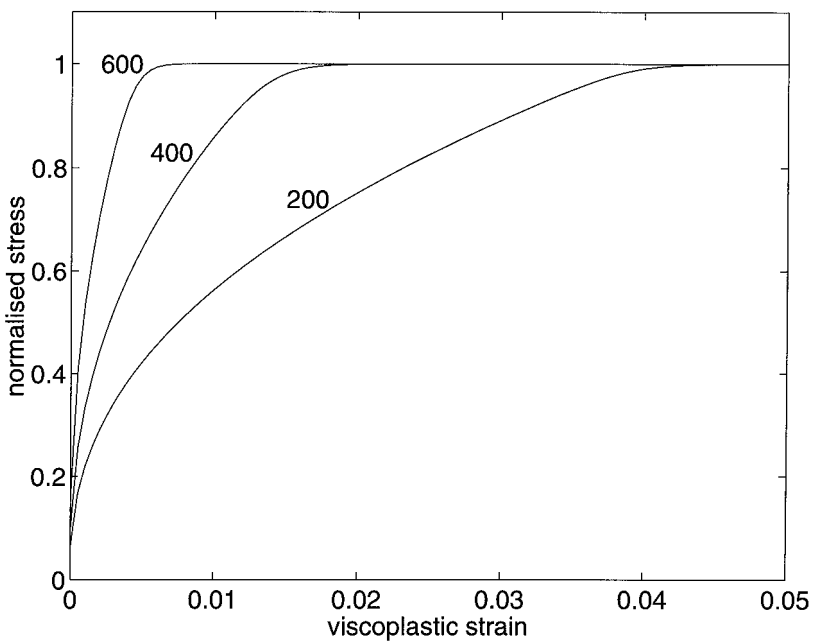


**Figure 6.** Stress (normalized by its steady-state value) *versus* viscoplastic strain for constant temperatures $T = 200$°C, 400°C, and 600°C and strain rate $10^{-4}$ $sec^{-1}$. The curves were produced by integrating the modified MATMOD equations.

temperature. In other words, the rheological behavior of the mushy zone does not induce strain hardening, although it might influence the final thermally induced deformations experienced by the ingot as well as the tendency toward hot tearing.

Gleeble measurements for determining the rheological behavior relevant for thermally induced deformations were recently performed on an AA3004 alloy by van Haaften et al. [24]. In this alloy, the content of silicon and magnesium is approximately 6 and 350 times, respectively, higher than in AA3103 studied in the present work. Van Haaften et al. subjected the specimens to a prestraining of 1 to 2% at various temperatures before they were strained at 50°C. It was found that prestraining at 400°C and 500°C did not change the low temperature behavior significantly, whereas prestraining at 300°C and below increased the yield stress level at 50°C. These results are in good agreement with the findings of the present work and indicate that the conclusions can be applied to other non-heat-treatable alloys as well as to the AA3103 alloy.

## CONCLUSION

- Gleeble tests with temperature and straining histories similar to those experienced by material points in the DC casting process as a consequence of thermal stresses have been applied to an AA3103 alloy in the as-cast condition.
- The measured stress was compared to the stress determined by a steady-state creep law, and they were found to correspond closely down to 400°C; the creep law increasingly overestimated the correct stress level as the temperature decreased further. At 300°C the creep law estimate can be as much as 43% higher than the measured stress, depending on the previous straining history.
- The results were discussed in view of common theories for strengthening mechanisms at high temperatures. In comparison with established internal variable constitutive equations it was argued that a steady-state creep law gives a better material description for temperatures above 400°C but that a more sophisticated material description is needed below this temperature.

## REFERENCES

1. J.-M. Drezet and M. Rappaz, Modelling of Ingot Distorsions during Direct Chill Casting of Aluminium Alloys, *Metal. Mat. Trans*., vol. 27A, pp. 3214–3225, October 1996.
2. J. Moriceau, Thermal Stresses in DC Casting of Al Alloys, in R. Rentsch (ed.), *Light Metals*, vol. 2, pp. 119–133, The Minerals, Metals & Materials Society, Warrendale, PA, 1975.
3. B. Janin, Simulation of Thermal Stresses in Continuous Casting of Al Alloys Billets, E-MRS meeting, p. 305, Strasbourg, 1986.
4. J. A. Danzig, Thermal Stress Development in Metal Casting Processes, *Metal. Sci. Tech*., vol. 7, pp. 133–178, 1989.
5. J. Mathew and H. D. Brody, Simulation of Thermal Stresses in Continuous Casting Using a Finite Element Method, *Nuclear Metal*., vol. 20, no. 2, pp. 978–990, 1976.
6. H. D. Brody, P. Wisniewskih, A. G. Gokhale, and J. Mathew, Tensile Behaviour of Solid Plus Liquid Alloys in Relation to Thermal Stress Analysis of Solidification Processes, in A. F. Giamei and G. J. Abbaschian (eds.), *Modeling and Control of Casting and Welding Processes IV*, pp. 351–360, The Minerals, Metals & Materials Society, Warrendale, PA, 1988.

7. H. G. Fjær and A. Mo, ALSPEN—A Mathematical Model for Thermal Stresses in D. C. Casting of Aluminium Billets, *Metal. Trans*., vol. 21B, pp. 1049–1061, 1990.
8. M. L. Nedreberg, Thermal Stress and Hot Tearing during the DC Casting of AlMgSi Billets, Ph.D. thesis, University of Oslo, February 1991.
9. B. Magnin, L. Katgerman, and B. Hannart, Physical and Numerical Modelling of Thermal Stress Generation during DC Casting of Aluminium Alloys, in M. Cross and J. Campbell (eds.), *Modelling of Casting, Welding and Advanced Solidification Processes—VII*, pp. 303–310, The Minerals, Metals & Materials Society, Warrendale, PA, 1995.
10. V. M. Sample and L. A. Lalli, Effects of Thermomechanical History on Hardness of Aluminium, *Mat. Sci. Tech*., vol. 3, pp. 28–35, 1987.
11. R. E. Smelser and O. Richmond, Constitutive Model Effects on Stresses and Deformations in a Solidifying Circular Cylinder, in A. F. Giamei and G. J. Abbaschian (eds.), *Modeling and Control of Casting and Welding Processes IV*, pp. 313–328, The Minerals, Metals & Materials Society, Warrendale, PA, 1988.
12. A. K. Miller, *Unified Constitutive Equations*, chap. 3, pp. 139–219, Elsevier Applied Science, New York, 1987.
13. H. G. Fjær and A. Håkonsen, The Mechanism of Pull-in during DC-casting of Aluminium Sheet Ingots, *TMS-Annual Meeting*, Orlando, FL, 1997.
14. F. Garofalo, An Empirical Relation Defining the Stress Dependence of Minimum Creep Rate in Metals, *Trans. TMS-AIME*, vol. 227, p. 351, 1963.
15. A. Mo and E. J. Holm, On the Use of Constitutive Internal Variable Equations for Thermal Stress Predictions in Aluminium Casting, *J. Thermal Stresses*, vol. 14, pp. 571–587, 1991.
16. H. G. Fjær and E. K. Jensen, Mathematical Modelling of Butt Curl Deformation of Sheet Ingots. Comparison with Experimental Results for Different Starting Block Shapes, in J. M. Evans (ed.), *Light Metals*, pp. 951–959, The Minerals, Metals & Materials Society, Warrendale, PA, 1995.
17. J.-M. Drezet, M. Rappaz, B. Carrupt, and M. Plata, Experimental Investigation of Thermomechanical Effects during Direct Chill and Electromagnetic Casting of Aluminum Alloys, *Metal. Mat. Trans*., vol. 26B, pp. 821–829, 1995.
18. I. Farup, J.-M. Drezet, A. Mo, and T. Iveland, Gleeble Machine Determination of Creep Law Parameters for Thermally Induced Deformations in Aluminium DC Casting, *J. Thermal Stresses*, vol. 23, pp. 47–58, 2000.
19. A. Mo, I. Farup, and J.-M. Drezet, Inhomogeneities in the Stress and Strain Rate Fields during Gleeble Testing, in J. L. Chenot, J. F. Agassant, P. Montmitonnet, B. Vergnes, and N. Billon (eds.), *First ESAFORM Conference on Material Forming*, Sophia Antipolis, France, March 1998.
20. H. G. Fjær, ALSPEN simulation results, private communication, 1998.
21. L. F. Mondolfo, *Aluminium Alloys: Structure and Properties*, Butter Worths, Boston, MA, 1976.
22. ASM International Handbook Committee (ed.), *Metals Handbook*, volume 2, 10th edition, ASM International, Materials Park, OH, 1990.
23. J. D. Verhoeven, *Fundamentals of Physical Metallurgy*, John Wiley & Sons, New York, 1975.
24. W. M. van Haaften, B. Magnin, W. H. Kool, and L. Katgerman, Thermomechanical Behaviour of an AA3004 Alloy at Low Strain Rate, in *Light Metals*, The Minerals, Metals & Materials Society, 1999.